J Membrane Biol (2015) 248:1159–1165
DOI 10.1007/s00232-015-9833-6

Dysfunction of Rice Mitochondrial Membrane Induced by Yb^{3+}

Jia-Ling Gao[1] · Man Wu[1] · Wen Liu[1] · Zhi-Jiang Feng[1] · Ye-Zhong Zhang[1] · Feng-Lei Jiang[2] · Yi Liu[1,2] · Jie Dai[1]

Received: 12 June 2015 / Accepted: 6 August 2015 / Published online: 25 August 2015

Abstract Ytterbium (Yb), a widely used rare earth element, is treated as highly toxic to human being and adverseness to plant. Mitochondria play a significant role in plant growth and development, and are proposed as a potential target for ytterbium toxicity. In this paper, the biological effect of Yb^{3+} on isolated rice mitochondria was investigated. We found that Yb^{3+} with high concentrations (200 $\sim$ 600 μM) not only induced mitochondrial membrane permeability transition (mtMPT), but also disturbed the mitochondrial ultrastructure. Moreover, Yb^{3+} caused the respiratory chain damage, ROS formation, membrane potential decrease, and mitochondrial complex II activity reverse. The results above suggested that Yb^{3+} with high concentrations could induce mitochondrial membrane dysfunction. These findings will support some valuable information to the safe application of Yb-based agents.

Keywords Yb^{3+} · Isolated mitochondria · Rice · Dysfunction

✉ Jie Dai
jiedai1969@126.com

[1] Department of Chemistry, College of Chemistry and Environmental Engineering, Yangtze University, Jingzhou 434023, Hubei, People's Republic of China

[2] State Key Laboratory of Virology & Key Laboratory of Analytical Chemistry for Biology and Medicine (MOE), College of Chemistry and Molecular Sciences, Wuhan University, Wuhan 430072, People's Republic of China

Introduction

As one of rare earth elements, Ytterbium is enablers for a wide range of industry development such as doping of stainless steel, dopant of active media, stress gauges, and so on (Gschneidner et al. 2002; Krishnamurthy and Gupta 2004). Owing to its special optic properties and chemical characteristics, the application of Ytterbium and its agents have gained significant awareness from some scientists as well. Ytterbium is used in cell imaging because of its NIR emission and chelation with some appropriate ligands, nitrate complexes for instance (Sues et al. 2012; Zhang et al. 2011). However, with the vast potential for future development, Ytterbium is apt to entering environment, causing abnormal distribution of positive Ytterbium in river, soil, and atmosphere (Potts et al. 1974).

The accumulation of Ytterbium in environment may inflict side effect on organism and living body, because its compounds are treated as highly toxic (Rim et al. 2013). So far, they are known to cause irritation to the human skin and eyes, and some might be teratogenic (Gale 1975). It could be accumulated in bones, kidney, and liver, which may cause some other serious problems. Some areas of China that located around rare earth mines have been labeled as "cancer villages," where the natives are vulnerable to cancer and orthopedic diseases. Ytterbium has a negative effect not only on human and animals but also on plants. In plant studies, Zhang found Yb_2O_3 NPs, Yb_2O_3, and $YbCl_3$ could inhibit the root elongation and plant growth, and the toxicity of Yb_2O_3 NPs may attributed to the internalization of Ytterbium into the cells (Zhang et al. 2012).

Some assays have indicated that rare earth elements could induce mitochondrial dysfunction (Gao et al. 2014; Zhao et al. 2013). Mitochondria are the center for plant

energy biology and play a vital role in the respiration and metabolism of plants. At mean time, mitochondria are the prime components of apoptotic machinery and sites of reactive oxygen species (ROS) generation. Owing to their role in the regulation of fundamental cellular functions, it is not surprising that mitochondria have been associated with plant growth and development.

Herein, we attempted to assess the effect of Yb^{3+} with different concentrations on rice mitochondria, including characteristic signals of mitochondrial membrane permeability transition (mtMPT), such as mitochondrial swelling, the disturbance of membrane potential, and fluidity. The mitochondrial function including succinate-linked respiratory chain, ROS generation, and complex II activity was investigated as well. Transmission electron microscope (TEM) was also applied to observe the ultrastructure changes of the rice mitochondria after loaded with Yb^{3+}.

Experiment Methods

Chemicals

Adenosine diphosphate (ADP), bovine serum albumin (BSA), 1,6-diphenyl-1,3,5-hexatriene (DPH), hematoporphyrin (HP), oligomycin, rhodamine 123 (Rh123), 2′,7′-dichlorofluorescein diacetate (DCFH-DA), 3-[4,5-dimethylthiazol-2-yl]-2,5-diphenyltetrazolium bromide (MTT), rotenone, and valinomycin were all purchased from Sigma (St. Louis, MO). All other reagents were of analytical grade, and all solutions were prepared using asepsis double-distilled water.

Mitochondrial Preparation

Hybrid Rice Fengyou 9 (purchased from Longping High-Tech Agriculture CO., Ltd. P. R. China) seedlings were grown in water at 35 °C in the dark with the water changed twice a day until it grew to a length of 9–10 cm long. Rice mitochondria were isolated by standard different centrifugation as previously described (Gao et al. 2014).

The rice tissue was minced with scissors, chilled on ice bath, and homogenized in buffer A containing 0.4 M sucrose, 1.0 mM EDTA, 30.0 mM Tris–HCl 4.0 mM cysteine, 0.6 % (g/mL) PVP, and 0.1 % (g/mL) BSA (pH 7.5). Then, the above solution was disrupted in a Waring blender at intermediate speed for 2 min and high speed for 2 min. After centrifuged the filtrate at $1500\times g$ for 10 min, the mitochondria were collected by centrifuging the supernatant at 11,000 g for 8 min. The purification of rice mitochondria was conducted by resuspending the mitochondria in about 50 mL buffer B containing 0.3 M sucrose, 1.0 mM EDTA, and 10.0 mM Tris–HCl (pH 7.5), and the thick mitochondria were then gained. The collection was further redistributed in buffer C containing 0.4 M sucrose, 0.3 M mannitol, and 50 mM Tris–HCl (pH 7.5). And finally, the supernatant was centrifuged at 11,000 g for 6 min. The purification of mitochondria was repeated for two times with same procedure as described above. All the above operations were performed aseptically at 0–4 °C. Mitochondrial protein was determined by Bradford method (Gornall et al. 1949).

Determination of Mitochondrial Swelling

Mitochondrial swelling was measured by monitoring the alterations of absorbance at 540 nm (Zhao et al. 2013). Mitochondria were suspended in 2 mL buffer C containing 250 mM sucrose, 20 mM HEPES, 2 mM $MgCl_2$, 5 mM KH_2PO_4, 20 mM succinate, and 1 μM rotenone (pH 7.2). The data were recorded for 10 min at room temperature with TU-1900 spectrophotometer.

Membrane Fluidity Assay in Isolated Mitochondria

Membrane fluidity changes were assessed by fluorescence excitation anisotropy of mitochondrial bound dyes (Richelli et al. 1999). Two probes were used: HP (6 μM, $\lambda_{ex} = 520$ nm; $\lambda_{em} = 626$ nm) and DPH (200 nM, $\lambda_{ex} = 340$ nm; $\lambda_{em} = 460$ nm). Mitochondria were dispersed in 2 mL buffer C with HP solution prepared in absolute ethanol or PDH solution in tetrahydrofuran. Anisotropic changes for HP were recorded by LS-55 fluorophotometer.

The anisotropy r is defined by the following equation:

$$r = (I_{II} - GI_{\perp})/(I_{II} + 2GI_{\perp}),$$

where I_{II} and $I_{\perp}$ are the fluorescence intensity polarized parallel and perpendicular to the vertical plane of polarization of the excitation beam, respectively. G represents the correction factor for instrumental artifacts with G equals to $I_{II}/I_{\perp}$ (Lakowicz 2007).

Mitochondrial Membrane Potential and ROS Generation by Flow Cytometry (FCM)

The change of mitochondrial transmembrane potential ($\Delta\Psi_m$) and ROS generation was monitored by Flow cytometry (Hosseini et al. 2013; Juan et al. 1994). Isolated mitochondrial fractions were incubated in buffer C with Rh123 (4 μM) or DCFH-DA (20 μM) at 37 °C for 20 min in the dark. Then, the pellets were incubated with different concentrations of Yb^{3+} for 5 min. The fluorescence of FL-1 channel was collected for at least 100,000 events with BD Accuri™ C6(BD, USA) and analyzed with BD Accuri™ C6 System software.

Assay of Mitochondrial Succinate-Linked Respiratory Chain

Mitochondrial succinate-linked respiratory chain measurement was monitored by a Clark oxygen electrode (Oxygraph; Hatchtech, Dorchester, UK) with magnetic stirring at 25 °C. Mitochondria were suspended in 1 mL respiration buffer solution, containing 250 mM sucrose, 20 mM KCl, 5 mM K_2HPO_4, 10 mM HEPES, 2 mM $MgCl_2$, and 1 μM rotenone (pH 7.0–7.4). State 4 respiration was initiated by adding 5 mM succinate, and state 3 was initiated by adding 5 mM succinate and 100 μM ADP into mitochondria buffer solution (Zhang et al. 2013).

Mitochondrial Complex II Activity by MTT Assay

The activity of mitochondrial complex II was assayed by measurement of reduction of MTT (Berridge and Tan 1993; Zhao et al. 2010). Briefly, 100 μL of mitochondria was incubated with varied concentration of Yb^{3+} at 37 °C for 10 min, then 0.5 % MTT was added to the solution and incubated at 37 °C for 30 min. The production formazan crystals were dissolved in 100 μL DMSO, and the absorbance at 570 nm was measured with microplate spectrophotometer (Biotek, ELx800, USA).

Mitochondria Ultrastructure

Mitochondria with variant concentrations of Yb^{3+} were fixed in glutaraldehyde at a final concentration of 2.5 % in 0.1 M cacodylate buffer for 45 min at 4 °C, and then postfixed with 1 % osmium tetroxide and dehydrated (Gzyl et al. 2009). The ultrastructure of mitochondria was observed with a JEM-100CX transmission electron microscope.

Results

Mitochondrial Swell Induce by Yb^{3+}

Mitochondrial swelling, reflecting the mtMPT, is a hallmark of mitochondrial dysfunction. The induction of mitochondrial swelling was assessed by observing the decreasing absorbance intensity of mitochondria at 540 nm. As shown in Fig. 1, different concentrations of Yb^{3+} could induce variant degree of mitochondrial swelling. Low concentrations (<200 μM) of Yb^{3+} have no obvious effect on mitochondria, while high concentrations (200–600 μM) promoted mitochondrial swelling in a concentration-dependent behavior.

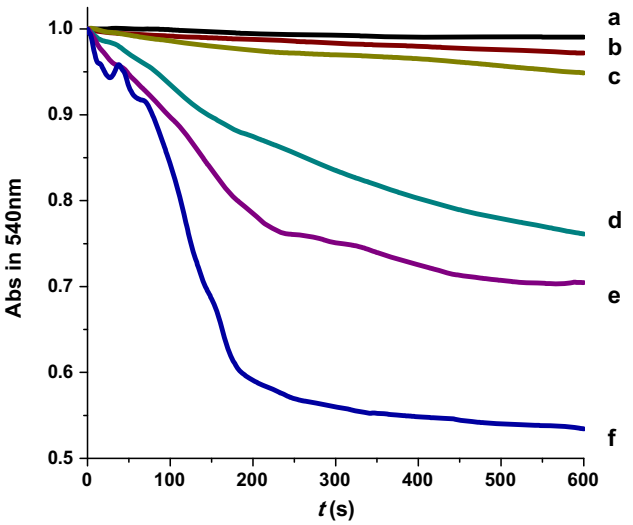

Fig. 1 Swelling of isolated rice mitochondria caused by various concentration of Yb^{3+}. $c(Yb^{3+})$/μM *a–f* 0, 50, 100, 200, 400, 600 (Color figure online)

The Changes of Mitochondrial Ultrastructure

To indicatively investigate the occurrence of MPT facilitated by Yb^{3+}, the ultrastructure of rice mitochondria exposed to different concentrations of Yb^{3+} was observed by TEM. As can be seen from Fig. 2a, mitochondria extracted from rice maintained their integrity, with a well-defined out-membrane, a narrow inter-membrane space, and compact cristae. With 100 μM Yb^{3+} loaded, the ultrastructure of mitochondria was some similar to the normal one except for the hardly distinguished cristae (Fig. 2b). However, with the treatment of 500 μM Yb^{3+}, mitochondria swelled with the appearance of a large inter-membrane space and the cristae clusters underwent a remarkably volume expansion (Fig. 2c).

Alteration of Mitochondrial Membrane Fluidity

Recent studies indicated that the induction of MPT often accompanied with the mitochondrial membrane fluidity change (Ricchelli et al. 2005). To determine what region of mitochondrial membrane Yb^{3+} was more susceptible to, HP and DPH fluorescence excitation anisotropy values were analyzed. HP mostly interacts with very polar, solvent-accessible regions of the lipid bilayer in liposomes, preferentially accumulates in protein regions of the inner membrane in mitochondria. While DPH mainly localizes in the hydrocarbon core and intercalates preferentially axial, between the acyl chains of the phospholipid bilayer (Fajardo et al. 2011).

The results in Fig. 3 showed, with the addition of Yb^{3+}, the florescence anisotropy of HP-labeled mitochondria was increased in a concentration-dependent mode, while the

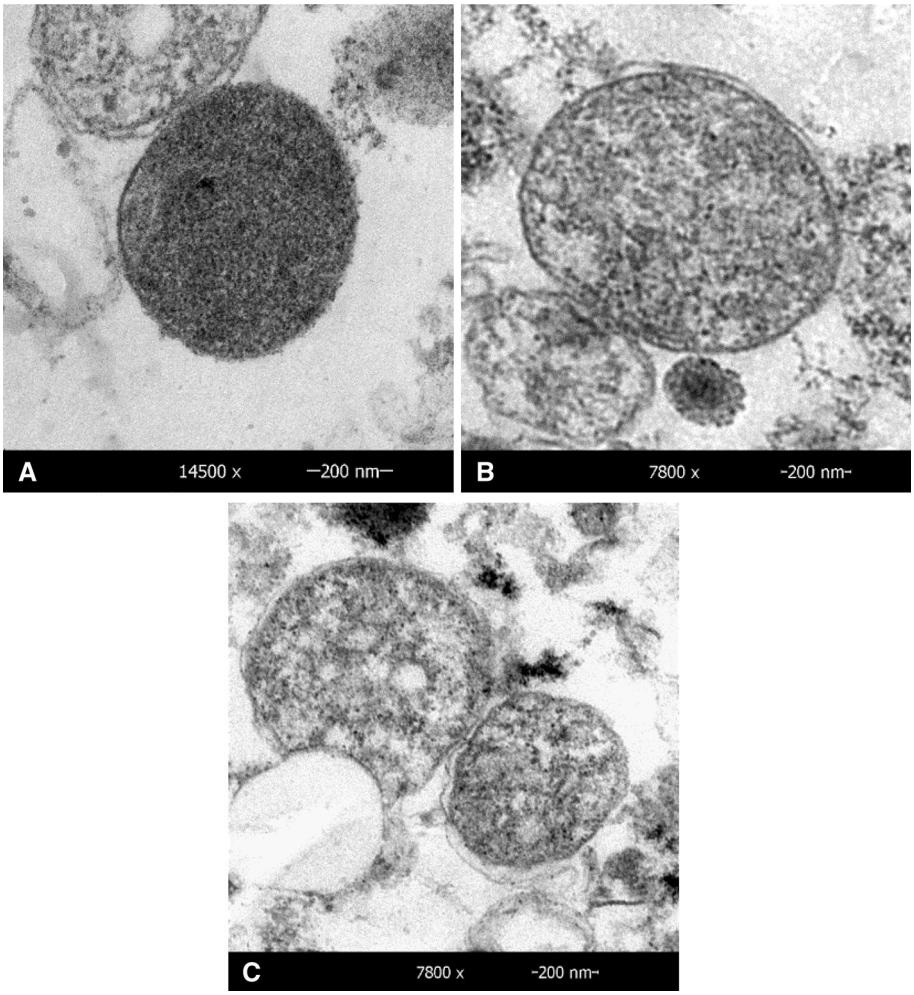

Fig. 2 Ultrastructure of mitochondria treated with 0 (**a**), 100 (**b**), and 500 μM Yb^{3+} (**c**)

florescence anisotropy change of DPH-labeled mitochondria was negligible. Here, the increase of HP anisotropy corresponds to the decrease of membrane fluidity. The results indicated that some proteins of mitochondrial membrane other than lipid bilayer were strongly disturbed after uptake of Yb^{3+}.

Effect of Yb^{3+} on Mitochondrial Potential and ROS Generation

In energized mitochondria, Rh123 accumulates in mitochondrial matrix due to the inside negative $\Delta\Psi$ of the mitochondrial inner membrane. In the case of membrane depolarization, Rh123 escaped from the mitochondria, resulting in the decrease of fluorescence intensity. As Fig. 4a shows, low concentrations of Yb^{3+} (<200 μM) enhanced membrane potential. However, when loaded with Yb^{3+} above the concentration of 200 μM, the membrane potential decreased notably. This indicated that Yb^{3+} with high concentrations could induce the dissipation of mitochondrial transmembrane potential.

DCFH-DA, a fluorescein-based bye, which is virtually non-fluorescent in the reduced state, becomes fluorescent after oxidation. Figure 3b shows that Yb^{3+} could rapidly accelerate mitochondrial ROS generation with increasing concentration of Yb^{3+}. But with 50 μM Yb^{3+}, this phenomenon was not obvious.

The Influence of Yb^{3+} on Succinate-Linked Respiratory Chain of Mitochondria

The influence of Yb^{3+} on succinate-linked respiratory chain of mitochondria was evaluated by polarography, with the complex II substrate succinate. At the physiological condition, the low respiratory rate of state 4 indicates an integrate mitochondrial inner membrane, which is vital to maintain the electrochemical proton potential at a high degree, and force the synthesis of ATP (Adlam et al. 2005). Meanwhile, a high respiratory rate of state 3 presents an intact electron transport chain and ATP synthase. In the presence of Yb^{3+}, the respiration rate of state 4 was stimulated, shown in Fig. 5, and the respiration rate of state 3 was increased by low

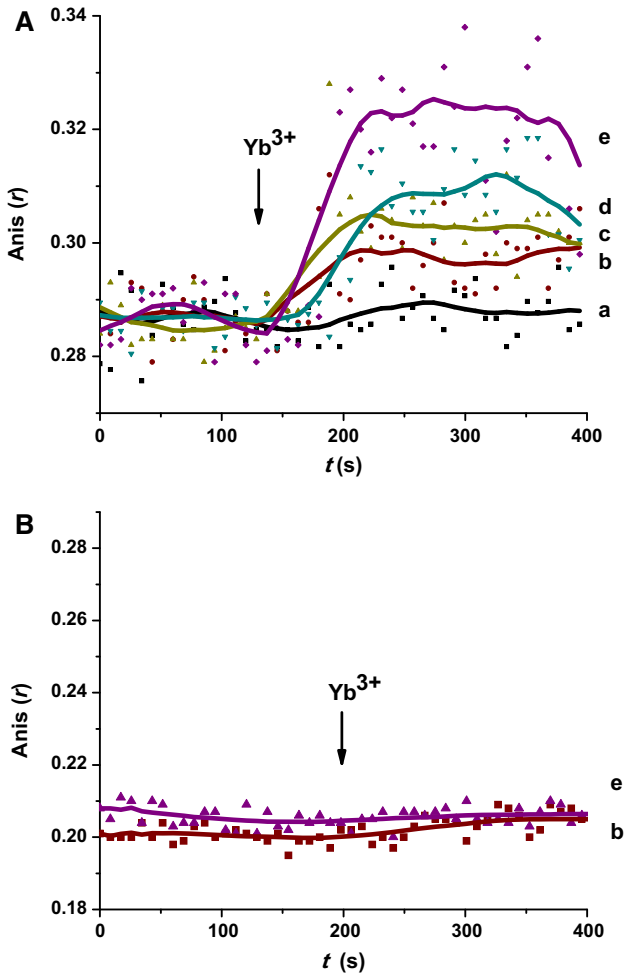

Fig. 3 Anisotropy changes of HP-labeled (**a**) and DPH-labeled (**b**) mitochondria. Changes were induced by the addition of different concentrations of Yb^{3+}. $c(Yb^{3+})$/μM *a–e* 0, 50, 100, 200, 400 (Color figure online)

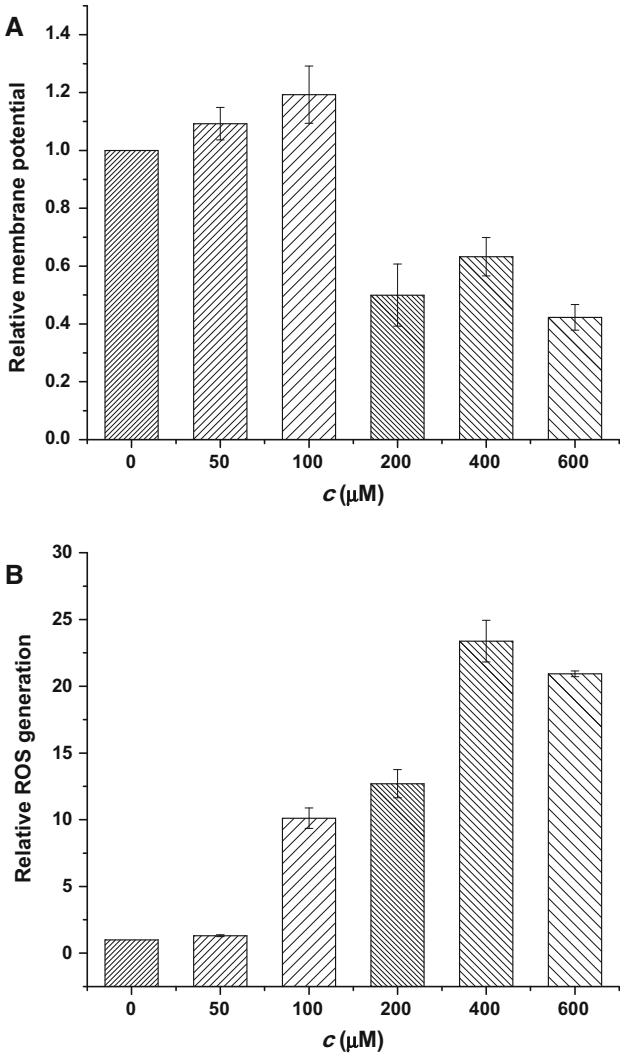

Fig. 4 **a** Effect of different concentrations of Yb^{3+} on mitochondrial membrane potential. **b** Yb^{3+} induced ROS generation of mitochondria. Data are the mean values of at least three individual experiments of the percent of recovery of fluorescence intensity relative to the change of fluoresce intensity without Yb^{3+}

concentrations of Yb^{3+} (<200 μM) and detracted rapidly by high concentrations (200–600 μM).

Respiratory control ratio (RCR), defined as the respiration rate of state 3 divided by that of state 4, is an important indicator to evaluate the mitochondrial oxidative phosphorylation and the membrane integrity. The high value occurs in the absence of Yb^{3+}. As shown in Fig. 5, Yb^{3+} facilitated mitochondrial dysfunction.

The Activity Variation of Mitochondrial Complex II

Succinate dehydrogenase (Complex II), acts as a prominent regulator of cell death, would inhibit succinate-linked respiratory chain, generate ROS, and further block the entire chain (Hwang et al. 2014). This implied that dissociation of complex II would lead to mitochondrial dysfunction. To clarify it, the complex II activity was determined by the MTT assay.

Under the experimental conditions, the mitochondria in the absence of Yb^{3+} or with a low concentration of Yb^{3+} (<200 μM) showed high activity, and the activity of isolated mitochondria was gradually reduced as the concentration of Yb^{3+} increased, which is shown in Fig. 6. This result indicated that Yb^{3+} with high concentrations (200–500 μM) led to a notable decrease in the complex II activity.

Discussion

As the primary organelle of ATP synthesis, mitochondria play a crucial role during the growth of plant and regulate various physiological and pathological phenomena

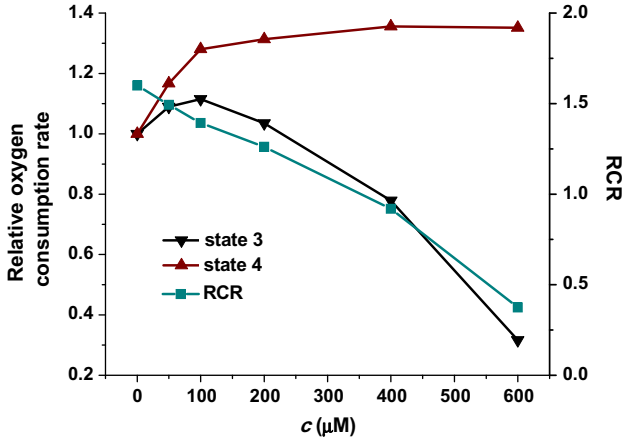

Fig. 5 Effect of Yb^{3+} on succinate-linked respiratory chain of isolated rice mitochondria. Respiratory control ratio (RCR = state 3/state 4)

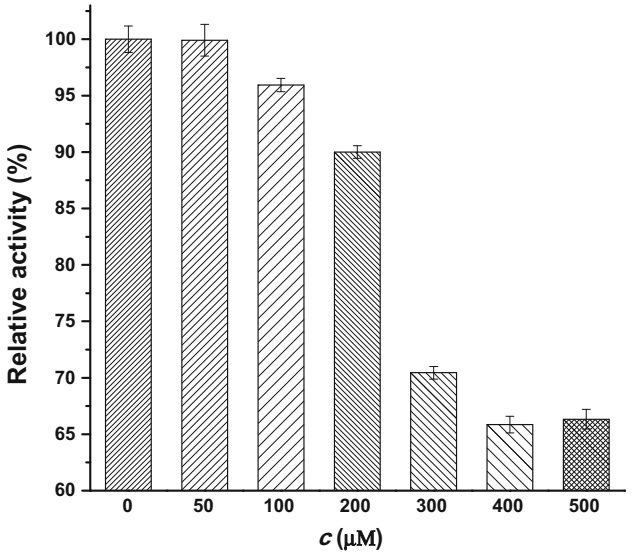

Fig. 6 Effect of Yb^{3+} on the activity of mitochondrial complex II

(Pourahmad and Hosseini 2012). The disorder of mitochondrial function will trigger the generation of ROS, release of cytochrome *c* to cytosol, finally leading to a wide range of cell death. Yb^{3+} cause cell death involving the mitochondria was reported in some publish (Liu et al. 2003). In this study, our work focused on the effect of Yb^{3+} on mitochondrial dysfunction. Our experimental phenomenon revealed that Yb^{3+} with high concentrations could induce mitochondrial swelling, collapse transmembrane potential, decrease membrane fluidity, facilitate ROS generation, restrain respiratory chain and inactive complex II, while Yb^{3+} with low concentration had little influence on mitochondria.

Mitochondrial swelling was associated with the mtMPT. When mtMPT happens, mitochondria undergo a sudden increase of permeability to solutes with molecular mass equal to or less than 1500 Da, resulting in the mitochondrial swelling (Crompton 1999; Di Lisa and Bernardi 2006; Gerencser et al. 2008; Halestrap et al. 2004; Tang et al. 2005). The obvious decrease of absorbance suggested exhibited Yb^{3+} could induce a mitochondrial swelling in a concentration-dependent manner (Fig. 1), which can be confirmed by the change of ultrastructure after treating with Yb^{3+}. Clearly seen in Fig. 2, the mitochondria treated with Yb^{3+} presented obvious difference with the intact one (Fig. 2a), suggesting the disturbance of mitochondrial membrane structure.

In the most cases, the mtMPT was accompanied with membrane fluidity change. The fluidity of HP-labeled mitochondria decreases with the addition of Yb^{3+} (Fig. 3a) rather than that of DPH-labeled mitochondria (Fig. 3b), indicating the inner membrane protein regions were strongly disturbed. Some researchers evaluated that lanthanides could chelate with protein (Lai et al. 2006). The complex II, one of the important protein complexes in the inner membrane, showed a reduced activity after uptake of high concentrations of Yb^{3+} (Fig. 6), which might have closed relevance with the membrane fluidity decrease.

Complex II is critical for the activity of electron transfer chain, and a prominent regulator of cell death (Hwang et al. 2014). Some assays illustrated that the generation of ROS results from complex II dissociation. Figure 4b confirms that Yb^{3+} with high concentrations (200–600 μM) stimulated ROS generation. H^+ is the crucial for keeping the function of respiratory chain at a normal range. With high concentrations of Yb^{3+} loaded, the membrane no longer maintains the electrochemical proton potential at a high degree. Thus, the membrane potential collapsed (Fig. 4a). Those two phenomena are in accordance with the results of mitochondrial respiratory chain (Fig. 5), which illustrated that Yb^{3+} could lead to mitochondrial dysfunction.

Conclusion

Our data collected from isolated rice mitochondria showed that Yb^{3+} with high concentration (200–600 μM) could induce transmembrane potential collapse and ROS generation, which was directly be involved in mitochondrial respiratory chain. Besides, the presence of Yb^{3+} also induced mtMPT, with series of phenomena such as swelling, membrane fluidity decrease, and inactive complex II. Meanwhile, Yb^{3+} with low concentration (<200 μM) had little influence on mitochondria.

Acknowledgments We gratefully acknowledge the financial support from the National Natural Science Foundation of China (Grant Nos. 21173026, 21225313) and Wuhan Yellow Crane Talents Plan of Science and Technology (2014).

References

Adlam VJ, Harrison JC, Porteous CM, James AM, Smith RA, Murphy MP, Sammut IA (2005) Targeting an antioxidant to mitochondria decreases cardiac ischemia-reperfusion injury. FASEB J 19:1088–1095

Berridge MV, Tan AS (1993) Characterization of the cellular reduction of 3-(4,5-dimethylthiazol-2-yl)-2,5-diphenyltetrazolium bromide (MTT): subcellular localization, substrate dependence, and involvement of mitochondrial electron transport in MTT reduction. Arch Biochem Biophys 303:474–482

Crompton M (1999) The mitochondrial permeability transition pore and its role in cell death. Biochem J 341:233–249

Di Lisa F, Bernardi P (2006) Mitochondria and ischemia–reperfusion injury of the heart: fixing a hole. Cardiovasc Res 70:191–199

Fajardo VA, McMeekin L, LeBlanc PJ (2011) Influence of phospholipid species on membrane fluidity: a meta-analysis for a novel phospholipid fluidity index. J Membr Biol 244:97–103

Gale TF (1975) The embryotoxicity of ytterbium chloride in golden hamsters. Teratology 11:289–295

Gao J-L, Wu M, Wang X, Zhang Y-Z, Jiang F-L, Liu Y, Dai J (2014) Membrane permeability transition and dysfunction of rice mitochondria effected by Er(III). J Membr Biol 248:39–46

Gerencser AA, Doczi J, Töröcsik B, Bossy-Wetzel E, Adam-Vizi V (2008) Mitochondrial swelling measurement in situ by optimized spatial filtering: astrocyte-neuron differences. Biophys J 95:2583–2598

Gornall AG, Bardawill CJ, David MM (1949) Determination of serum proteins by means of the biuret reaction. J Biol Chem 177:751–766

Gschneidner KA, Eyring L, Lander GH (2002) Handbook on the physics and chemistry of rare earths, vol 32. Elsevier, Amsterdam

Gzyl J, Przymusiński R, Gwóźdź EA (2009) Ultrastructure analysis of cadmium-tolerant and-sensitive cell lines of cucumber (*Cucumis sativus L.*). Plant Cell Tissue Organ Cult 99:227–232

Halestrap AP, Clarke SJ, Javadov SA (2004) Mitochondrial permeability transition pore opening during myocardial reperfusion—a target for cardioprotection. Cardiovasc Res 61:372–385

Hosseini M-J, Shaki F, Ghazi-Khansari M, Pourahmad J (2013) Toxicity of vanadium on isolated rat liver mitochondria: a new mechanistic approach. Metallomics 5:152–166

Hwang M-S, Rohlena J, Dong L-F, Neuzil J, Grimm S (2014) Powerhouse down: complex II dissociation in the respiratory chain. Mitochondrion 19:20–28

Juan G, Cavazzoni M, Saez GT, O'Connor JE (1994) A fast kinetic method for assessing mitochondrial membrane potential in isolated hepatocytes with rhodamine 123 and flow cytometry. Cytometry 15:335–342

Krishnamurthy N, Gupta CK (2004) Extractive metallurgy of rare earths. CRC Press, Boca Raton

Lai Y, Wang Q, Yang L, Huang B (2006) Subcellular distribution of rare earth elements and characterization of their binding species in a newly discovered hyperaccumulator Pronephrium simplex. Talanta 70:26–31

Lakowicz JR (2007) Principles of fluorescence spectroscopy. Springer, Berlin

Liu H, Yuan L, Yang X, Wang K (2003) La^{3+}, Gd^{3+} and Yb^{3+} induced changes in mitochondrial structure, membrane permeability, cytochrome c release and intracellular ROS level. Chem Biol Interact 146:27–37

Potts MJ, Lee CW, Cadieux JR (1974) Rare earth element composition of atmospheric particulates. Environ Sci Technol 8:585–587

Pourahmad J, Hosseini M-J (2012) Application of isolated mitochondria in toxicological and clinical studies. Iran J Pharm Res 11:703

Ricchelli F, Gobbo S, Moreno G, Salet C (1999) Changes of the fluidity of mitochondrial membranes induced by the permeability transition. Biochemistry 38:9295–9300

Ricchelli F, Dabbeni-Sala F, Petronilli V, Bernardi P, Hopkins B, Bova S (2005) Species-specific modulation of the mitochondrial permeability transition by norbormide. Biochim Biophys Acta 1708:178–186

Rim KT, Koo KH, Park JS (2013) Toxicological evaluations of rare earths and their health impacts to workers: a literature review. Saf Health Work 4:12–26

Sues PE, Lough AJ, Morris RH (2012) Synthesis, characterization, and activity of yttrium (III) nitrate complexes bearing tripodal phosphine oxide and mixed phosphine-phosphine oxide ligands. Inorg Chem 51:9322–9332

Tang X et al (2005) Inhibition of ursolic acid on calcium-induced mitochondrial permeability transition and release of two proapoptotic proteins. Biochem Biophys Res Commun 337:320–324

Zhang T et al (2011) Water-soluble mitochondria-specific ytterbium complex with impressive NIR emission. J Am Chem Soc 133:20120–20122

Zhang P et al (2012) Comparative toxicity of nanoparticulate/bulk Yb_2O_3 and $YbCl_3$ to cucumber (*Cucumis sativus*). Environ Sci Technol 46:1834–1841

Zhang Y, Tian F, Xiao Q, Hu Y, Li J, Jiang F, Liu Y (2013) Exploiting the role of resveratrol in rat mitochondrial permeability transition. J Membr Biol 246:365–373

Zhao Y, Ye L, Liu H, Xia Q, Zhang Y, Yang X, Wang K (2010) Vanadium compounds induced mitochondria permeability transition pore (PTP) opening related to oxidative stress. J Inorg Biochem 104:371–378

Zhao J et al (2013) High concentration of gadolinium ion modifying isolated rice mitochondrial biogenesis. Biol Trace Elem Res 156:308–315